Molecular Biology of the Cell
Vol. 12, 2578–2589, September 2001

Dynamin GTPase Domain Mutants Block Endocytic Vesicle Formation at Morphologically Distinct Stages

Hanna Damke,* Derk D. Binns,† Hideho Ueda,‡ Sandra L. Schmid,*§ and Takeshi Baba‡

*Department of Cell Biology, The Scripps Research Institute, La Jolla, California 92037; †Department of Pharmacology, University of Texas Southwestern Medical Center, Dallas, Texas 75390; ‡Department of Anatomy, Yamanashi Medical University, 1110 Shimokato, Tamaho, Yamanashi 409-3898, Japan

Submitted March 21, 2001; Revised May 15, 2001; Accepted July 2, 2001
Monitoring Editor: Suzanne R. Pfeffer

Abundant evidence has shown that the GTPase dynamin is required for receptor-mediated endocytosis, but its exact role in endocytic clathrin-coated vesicle formation remains to be established. Whereas dynamin GTPase domain mutants that are defective in GTP binding and hydrolysis are potent dominant-negative inhibitors of receptor-mediated endocytosis, overexpression of dynamin GTPase effector domain (GED) mutants that are selectively defective in assembly-stimulated GTPase-activating protein activity can stimulate the formation of constricted coated pits and receptor-mediated endocytosis. These apparently conflicting results suggest that a complex relationship exists between dynamin's GTPase cycle of binding and hydrolysis and its role in endocytic coated vesicle formation. We sought to explore this complex relationship by generating dynamin GTPase mutants predicted to be defective at distinct stages of its GTPase cycle and examining the structural intermediates that accumulate in cells overexpressing these mutants. We report that the effects of nucleotide-binding domain mutants on dynamin's GTPase cycle in vitro are not as predicted by comparison to other GTPase superfamily members. Specifically, GTP and GDP association was destabilized for each of the GTPase domain mutants we analyzed. Nonetheless, we find that overexpression of dynamin mutants with subtle differences in their GTPase properties can lead to the accumulation of distinct intermediates in endocytic coated vesicle formation.

INTRODUCTION

The clathrin-dependent pathway of receptor-mediated endocytosis is a multistep process. Clathrin-coated vesicle formation is initiated by the binding of coat components to nucleation sites at the plasma membrane (Kirchhausen, 1999, 2000). Driven by coat assembly and perhaps by rearrangements of the coat constituents, the initially flat clathrin lattice gains curvature and forms an increasingly invaginated coated pit. The neck of the coated pit becomes constricted before the fission reaction that leads to release of the coated vesicle (Schmid, 1997). The large GTPase dynamin (dyn) is required for clathrin-mediated endocytosis (reviewed by Hinshaw, 2000), but the mechanistic details of its role in vesicle formation remain controversial (Roos and Kelly, 1997; Sever *et al.*, 2000b).

Dyn is a member of a subfamily of functionally diverse, high molecular weight GTPases, which have atypically low affinities for GTP and high intrinsic rates of GTP hydrolysis. Dyn (and other dyn family members) spontaneously self-assembles in vitro into single rings and spirals upon dilution into low ionic strength buffers (Hinshaw and Schmid, 1995) or in the presence of artificial templates such as microtubules or phosphatidylinositol 4,5-bisphosphate-containing phospholipid vesicles (Shpetner and Vallee, 1989; Barylko *et al.*, 1998; Stowell *et al.*, 1999). Self-assembly stimulates dyn's basal GTPase activity 10- to 100-fold (Tuma and Collins, 1994; Warnock *et al.*, 1996), and GTP hydrolysis drives dyn disassembly (Maeda *et al.*, 1992; Warnock *et al.*, 1997). It is not known whether other factors, in addition to self-assembly, are required to regulate dyn's GTPase activity in vivo.

Dyn's function in endocytosis was initially suggested when electron microscopy (EM) of nerve terminals in *Drosophila* bearing a temperature-sensitive allele of the dyn ho-

§ Corresponding author. E-mail address: slschmid@scripps.edu.

Abbreviations used: Ad, adenovirus; BSS-Tfn, biotinylated Tfn; dyn, dynamin; EM, electron microscopy; GAP, GTPase-activating protein; GED, GTPase effector domain; HA, hemagglutinin; Mant-GDP, 2′deoxy-3′*O*-*N*-methylanthraniloyl GDP; Mant-GNP, 2′deoxy-3′*O*-*N*-methylanthraniloyl GNP; Mant-GTP, 2′deoxy-3′*O*-*N*-methylanthraniloyl GTP; MOI, multiplicity of infection; PBS, phosphate-buffered saline; tet, tetracycline; Tfn, transferrin; tTA, transactivator; WT, wild type.

mologue *shibire* revealed the accumulation of endocytic pits. Most of the pits accumulating on presynaptic membranes were encircled at their necks by a single or double electron-dense band of dimensions similar to dyn rings (Koenig and Ikeda, 1989). Importantly, although endocytosis is blocked in all tissues of the fly, dyn "collars" have been detected only in neuronal cells. In most cells in *shibire* flies and in mammalian cells overexpressing the human homologue of the shibire^{ts-1} allele, dyn(G273D), or a dominant-negative mutant of dyn defective in GTP binding and hydrolysis, dyn(K44A), inhibition of endocytosis leads to the accumulation of invaginated coated pits with necks that remain open to bulky probes such as avidin (Damke *et al.*, 1994; Damke *et al.*, 1995a).

When dyn is assembled around lipid templates, GTP hydrolysis induces a conformational change. Depending on the composition of the lipid, this conformational change can cause either constriction of the dyn spirals resulting in vesiculation (Sweitzer and Hinshaw, 1998) or an increase in the distance between the rungs of the assembled dyn spiral (Stowell *et al.*, 1999). Together these in vitro observations have led to a variety of working models proposing that dyn functions as a mechanochemical enzyme (Hinshaw and Schmid, 1995; Warnock and Schmid, 1996; Smirnova *et al.*, 1999; Stowell *et al.*, 1999; Kozlov, 2001; for review, see Sever *et al.*, 2000b). Although differing significantly in their details, these models all suggest that dyn's high, assembly-stimulated rate of GTP hydrolysis would be required for pinching off vesicles from the plasma membrane.

Several laboratories have indeed established that overexpression of dyn GTPase domain mutants defective in GTP binding and/or hydrolysis inhibits endocytosis in mammalian cells (Herskovits *et al.*, 1993; van der Bliek *et al.*, 1993; Hill *et al.*, 2001; Marks *et al.*, 2001). However, contradictory results were obtained with the use of dyn GTPase effector domain (GED) mutants. GED is an intramolecular GTPase-activating protein (GAP) that is required for dyn's assembly-stimulated GTPase activity but not for its basal rate of GTP binding and hydrolysis (Sever *et al.*, 1999). Overexpression of these GAP-impaired dyn mutants accelerates the rate-limiting step in endocytosis leading to an increase in the rate of formation of constricted coated pits (Sever *et al.*, 1999, 2000a). Depending on the specific GED mutant, this can, in turn, lead to an increased rate of receptor-mediated endocytosis. Together, these data suggest a complex relationship between dyn's GTPase cycle, its regulation, and the execution of distinct stages in the formation of clathrin-coated vesicles.

As a means to explore this complex relationship we sought to use the overexpression of dyn mutants defective in distinct steps of its GTPase cycle to accumulate sequential intermediates of clathrin-coated vesicle formation. The dyn mutants were designed in analogy to other members of the GTPase superfamily and were predicted to arrest dyn in its GDP-bound, GTP-bound, or nucleotide-unoccupied state. Biochemical characterization of these mutants revealed unexpected results relating to their GTPase properties in that neither of the mutations resulted in a GTPase predicted to be "locked" in either the activated or inactivated state. The formation of constricted coated pits was inhibited by the dyn GTPase domain mutants that we generated; however, quantitative morphological analysis revealed subtle differences in the intermediates that accumulated.

MATERIALS AND METHODS

Reagents

The mouse monoclonal anti-transferrin (Tfn) receptor antibody HTR.D65 was a kind gift from I. Trowbridge (Salk Institute, La Jolla, CA). Rhodamine-conjugated Tfn was purchased from Molecular Probes (Eugene, OR). Human differric Tfn was from Roche Molecular Biochemicals (Indianapolis, IN). Tfn was biotinylated as previously described (Smythe *et al.*, 1992). Colloidal gold (5 and 10 nm) and all other reagents used for EM were purchased from Electron Microscopy Sciences (Fort Washington, PA). D65 was conjugated to gold after standard protocols (Leunissen and DeMey, 1987). All other chemicals were reagent grade, unless otherwise specified.

Preparation of cDNA Constructs

The point mutations for N-terminal hemagglutinin (HA)-tagged dyn K44A (Damke *et al.*, 1994), S45N, and T65F were introduced into the wild-type (WT) human dyn-1 by site-directed mutagenesis with polymerase chain reaction and verified by DNA sequencing. The mutant cDNAs were then subcloned into expression vectors for the generation of tetracycline (tet)-regulatable stable cell lines, pUHD10–3, (Gossen and Bujard, 1992; Damke *et al.*, 1995b) or recombinant adenovirus (Ad), pADT3T7 (Hardy *et al.*, 1997).

Generation of Stably Transformed Cells

The stable HeLa cell line, tTA-HeLa, expressing the chimeric tet-regulatable transcription activator was kindly provided by H. Bujard (Zentrum für Molekulare Biologie der Universität, Heidelberg, Germany). Cells were maintained in DMEM supplemented with 10% (vol/vol) fetal bovine serum, 100 U/ml each penicillin and streptomycin, and 400 μg/ml active G418 (Geneticin; GIBCO BRL, Gaithersburg, MD). The constructs pUHD10–3 encoding HA-tagged dyn(S45N), dyn(T65F), and dyn(D208N) were used to generate stably transformed tTA-HeLa cells with tightly regulated expression of dyn as previously described (Damke *et al.*, 1995b). Puromycin was used as a selectable marker. Stably transformed cells were cultured in the presence of 1 μg/ml tet and induced by the removal of tet by two washes with phosphate-buffered saline (PBS) and incubating the cells in growth medium without tet for 48 h.

Ad Generation

Recombinant viruses for dyn-1 (Ad-Dyn1) were generated as previously described (Hardy *et al.*, 1997; Altschuler *et al.*, 1998). Briefly, WT and mutant dyn-1 were placed under the control of a tet-regulatable promotor in the pAdlox vector by inserting the coding sequence between the ψ5-packaging site and the 5′-polyA site. These constructs were then cotransfected into HEK293 cells expressing Cre recombinase. Ad was plaque purified and amplified in HEK 293 cells.

Immunoblot Analysis

For quantification of dyn expression, cell lysates of equivalent numbers of cells were prepared for WT and all dyn mutants and analyzed by immunoblotting. For reliable quantification different amounts of the cell lysates for all samples were separated on SDS gels. The pan-dyn antibody 748 (van der Bliek *et al.*, 1993) was used to detect dyn in comparison with endogenous dyn in uninduced cells, and the anti-HA antibody 12CA5 (Roche Molecular Biochemicals) was used to quantify matching expression levels in HA-dyn-1–overexpressing cells. Antigen-antibody complexes were visual-

ized with the use of alkaline phosphatase, and the bands were quantified by densitometry.

Internalization Assays

Stably transformed tTA-HeLa cells expressing dyn-1 WT or mutants were grown in the presence or absence of tet for ~48 h to ~60% confluency. Alternatively tTA-HeLa cells were infected with Ad (10 MOI/cell) encoding either wild-type (WT) or mutant dyn-1 (Ad-dyn^{WT}, Ad-dyn^{K44A}, Ad-dyn^{S45N}, Ad-dyn^{T65F}). The cells were detached with PBS and 5 mM EDTA at room temperature for 5 min, briefly rinsed, and resuspended in ice-cold PBS containing 1 mM $MgCl_2$, 1 mM $CaCl_2$, 0.2% bovine serum albumin, and 5 mM glucose (PBS^{++++}) at 2×10^6 cells/ml. BSS-Tfn was added to the suspension to a final concentration of 8 μg/ml BSS-Tfn and kept on ice. The cell suspension was then split into 50-μl aliquots (corresponding to 1×10^5 cells) for continuous internalization of BSS-Tfn at 37°C for the indicated times. Endocytosis was terminated by returning the samples to ice and addition of 1 ml of ice-cold PBS^{++++}. Internalization was quantified after processing the samples for measuring avidin inaccessibility or MesNa (2-mercaptoethanesulfonic acid) resistance as described by Carter *et al.* (1993). Internalized BSS-Tfn was expressed as the percentage of total surface-bound BSS-Tfn at 4°C.

Transmission EM

For conventional Epon sections, stably transformed cells were induced for 48 h in the absence of tet and grown to <75% confluency on 12-mm glass coverslips. Alternatively, tTA-HeLa cells were infected with Ad for WT or mutant dyn-1 (Ad-dyn^{WT}, Ad-dyn^{K44A}, Ad-dyn^{S45N}, Ad-dyn^{T65F}) and incubated in the absence of tet for 16 h. The expression level of recombinant protein was controlled for by immunoblot analysis (12CA5 anti-HA antibody) of equivalent numbers of cells. Adenoviral infection itself did not affect overall cell morphology or the appearance of coated pits. Cells were incubated with D65-gold (10 nm) in PBS^{++++} for 120 min at 4°C and warmed for 2 min at 37°C. The cells were then washed and fixed in 2% glutaraldehyde in 100 mM sodium cacodylate buffer, pH 7.4, for 30 min at room temperature. Subsequently the coverslips were washed for 1 h at room temperature in 100 mM sodium cacodylate buffer, pH 7.4 (four changes). The samples were postfixed with 1% OsO_4, 1% potassium ferrocyanide, and 100 mM sodium cacodylate buffer, pH 7.4, for 1 h on ice, washed with four changes of distilled H_2O at room temperature, and stained with 2% uranyl acetate for 1 h at room temperature. After three washes in distilled H_2O at room temperature the samples were dehydrated and embedded in Epon following standard protocols. Ultrathin sections were observed under an electron microscope (model CM10; Philips Electronic Instruments, Mahwah, NJ) at 80 kV. At the same time, low magnification (5000×) images of cells were captured with a slow-scan charge-coupled device camera, and their perimeters were measured with the use of National Institutes of Health image software. Quantitation of coated pit accumulation was performed by photographing individual cell profiles at low magnification (5000×) to measure surface length on negatives and then counting the number of coated pits and classifying their morphology at high magnification (19,000×). Twenty cell profiles were counted for each condition. Shallow pits were defined as having fully open mouths and u-shaped openings; deeply curved pits had narrow openings and were "omega" shaped; sealed pits were completely encircled by coated membrane. Serial section analysis revealed that almost all sealed pits were connected to the cell surface in neighboring sections; therefore, they were grouped into the category of deep coated pits. Gold particles located on coated versus noncoated regions of the cell surface were also counted. The dimensions of randomly photographed deeply curved or sealed pits having clearly defined diameters were measured on EM negatives at 21,000× with the use of a 15× magnifying glass and a ruler with 0.1-mm subdivisions.

For labeling of invaginated membranes with Ruthenium red, tTA-HeLa cells were cultured on 12-mm glass coverslips. The cells were infected with Ad for WT or mutant dyn-1 and incubated in the absence of tet for 16 h. The cells were fixed for 1 h with 1.2% glutaraldehyde in 0.1 M HEPES, pH 7.2, containing 0.5 mg/ml Ruthenium red at room temperature. The cells were rinsed three times with 0.1 M HEPES and postfixed for 4 h with 1.6% OsO_4 in 0.1 M HEPES, pH 7.2, containing 0.5 mg/ml Ruthenium red at room temperature. These specimens were routinely embedded in Epon, and unstained ultrathin sections were observed under an electron microscope (model H-7500; Hitachi, Tokyo, Japan) at 80 kV.

Sedimentation Assays and GTPase Assays

Recombinant WT and mutant dynamins were purified from Baculovirus-infected TNS cells, as previously described (Damke *et al.* 2001). Velocity sedimentation assays were performed as previously described (Warnock *et al.*, 1996; Damke *et al.*, 2001). GTPase activity was determined at 37°C with the use of [α-^{32}P]GTP in 20 mM HEPES, pH 7.2, mM EGTA, 1 mM $MgCl_2$, 52 mM NaCl, 1 mM dithiothreitol, 0.1% bovine serum albumin, and 0.5 mM GTP and in the presence or absence of either GED or microtubules exactly as previously described (Sever *et al.*, 1999; Damke *et al.*, 2001).

Stop Flow Measurements

Stop-flow measurements were perfomed with an SFM-3 instrument (BioLogicals, Toronto, Canada) fitted with an FC-15 cuvette (1.5-mm path length) in the "hard stop" mode. The flow velocity was 6 ml/s. Excitation was at 280 nm from a 150-W Hg/Ze arc lamp through a monochromator. Emitted light was detected with a photomultiplier through a 395-nm cut-off filter (50% transmission at 400 nm, <1% at 360 nm; catalog number 51271; Oriel Corp, Stamford, CT) set at 90° to the incident light (fluorescence mode). Data from the SFM-3 were analyzed with the use of Biokine (BioLogicals) software.

To measure the 2′deoxy-3′*O*-*N*-methylanthraniloyl GNP (Mant-GNP) on rate for each reaction, one syringe containing 2.0 μM protein and one containing 120 μM Mant-GNP were prepared. Equal volumes were simultaneously injected from each syringe into the cuvette bringing the final protein concentration to 1.0 μM and the final GNP concentration to 60 μM. The mixture was excited at 280 nm (to excite the tryptophans in dyn), and the fluorescence emission was collected above 395 nm with the use of a cut-off filter. Mant absorbs at 360 nm, where tryptophan emits when excited at 280 nm (resulting in excitation of the mant by any tryptophans in dyn that are spatially close to the mant group). Mant emits at 410 nm. The Mant-GNP cut-off rates were determined as follows: one syringe was loaded with 2 μM protein and 8 μM Mant-GNP. A second syringe was loaded with 200 μM unlabeled (cold) GTP. Equal volumes were mixed from each syringe in the cuvette, and the reaction was monitored in the same way as for the on rates. The final concentrations of protein, Mant-GNP, and cold GTP were 1, 4, and 100 μM, respectively.

RESULTS

That dyn functions in clathrin-coated vesicle formation and receptor-mediated endocytosis is well documented, but its exact role remains to be established. Based largely on dyn's biochemical properties in vitro (Hinshaw and Schmid, 1995; Sweitzer and Hinshaw, 1998; Stowell *et al.*, 1999), many of the prevailing models suggest that it functions late in endocytic vesicle formation to drive membrane fission (for reviews, see McNiven, 1998; Hinshaw, 2000; Sever *et al.*, 2000b). More recent in vivo results have suggested that dyn might also, or instead, regulate earlier events in endocytic coated vesicle formation (Shupliakov *et al.*, 1997; Sever *et al.*, 2000a; Hill *et al.*, 2001). Other GTPase superfamily members,

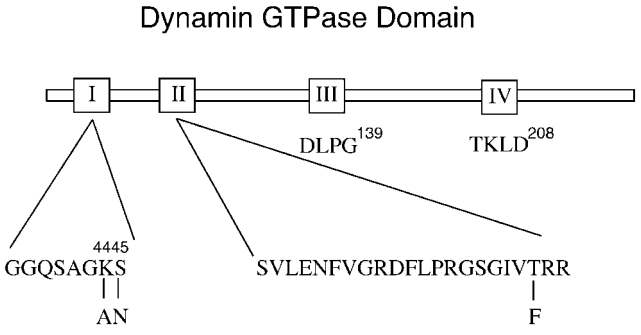

Figure 1. Mutations within dyn GTPase domain. Point mutations were introduced within the nucleotide-binding region to interfere with dyn's nucleotide-binding properties and biological function. Shown are the positions of the mutations within the first of three GTP-binding elements conserved among GTPase family members.

e.g., rab proteins, regulate multiple events in vesicular trafficking as they cycle between their GTP- and GDP-bound conformations. To better understand the function of dyn's GTPase cycle in regulating endocytic vesicle formation in vivo, we introduced point mutations within the nucleotide-binding regions of the GTPase domain (Figure 1) predicted to generate dyn mutants that preferentially adopt the GTP-, GDP-, or nucleotide-unoccupied states. Specifically, Ser45, an invariant residue located in the first GTP-binding element or "P-loop" coordinates with Mg^{2+}, which in turn binds to the γ- and β-phosphate of the bound nucleotide (Wittinghofer, 2000). Substitution with Asn lowers the affinity for GTP more than GDP and in many cases results in a GTPase restricted to the GDP-bound state (reviewed by Olkkonen and Stenmark, 1997; Wittinghofer, 2000). The second GTP-binding element, also known as the "switch 1" region, has the less well defined sequence, D-$(X)_n$-T, in which the conserved Thr is predicted to coordinate with the Mg^{2+} ion necessary for GTP hydrolysis but not for GTP binding (Bourne *et al.*, 1991). Dyn has three D-$(X)_n$-T motifs between the first and third well defined GTP-binding elements encompassing Thr65, Thr109, and Thr 133. Each of these Thr residues was replaced with phenylalanine, but only mutation of Thr65 generated a GTPase-defective mutant (see below and Damke, unpublished results), thus identifying this residue as a constituent of the second GTP-binding element, as previously predicted (van der Bliek, 1999). The K44A dyn mutant was generated earlier and has been shown to exhibit a substantially reduced affinity for GTP and reduced GTP hydrolysis (Damke *et al.*, 1994; Warnock *et al.*, 1995).

Biochemical Characterization of the Point Mutations dyn(S45N) and dyn(T65F)

To test directly whether the new dyn mutants that we designed exhibited the predicted biochemical properties, recombinant baculoviruses were generated enabling expression and purification of WT and mutant proteins. Dyn's GTPase activity is closely linked to its ability to self-assemble (Warnock *et al.*, 1996; Binns *et al.*, 1999). Therefore, although the point mutations are only predicted to interfere with dyn's GTPase activity, we first compared the mutants'

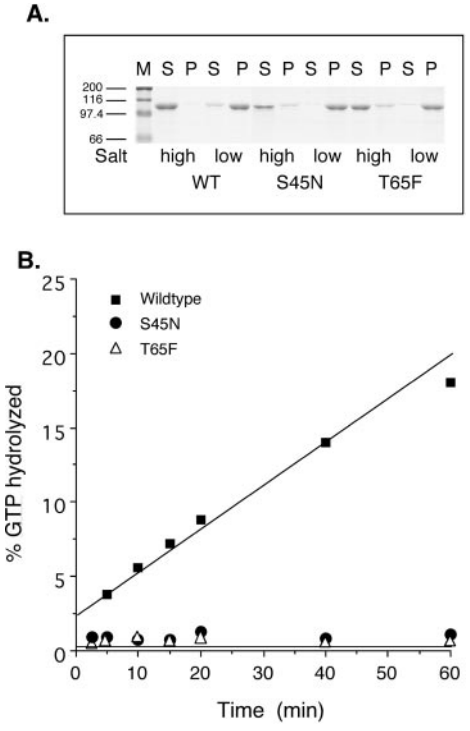

Figure 2. Biochemical characteristics of dyn GTPase domain mutants. (A) A sedimentation assay, described in MATERIALS AND METHODS, was used to analyze the ability of S45N and T65F mutant dyn compared with WT dyn to self-assemble into structures that remain soluble (S) or pelletable (P) after dilution into low salt conditions. The self-assembly activity of dyn(S45N) and dyn(T65F) was indistinguishable from dyn(WT). M=marker. (B) The assembly-stimulated GTPase activity of WT and mutant dyns was measured, as described in MATERIALS AND METHODS, with the use of taxol-stabilized microtubules (2 μg) as a template for assembly. GTPase activity of dyn(K44A), dyn(S45N), and dyn(T65F) was severely impaired relative to dyn(WT).

ability to self-assemble into sedimentable higher order structures under low ionic conditions. Previous studies had established that dyn(K44A) retained its ability to self-assemble (Warnock *et al.*, 1996). Similarly, the data in Figure 2A show that the assembly activity of dyn(S45N) and dyn(T65F) were also indistinguishable from dyn(WT).

We next confirmed the predicted GTPase defect in the various mutants. As expected, we were unable to detect basal, unstimulated GTPase activity for either dyn(S45N) or dyn(T65F). Similarly, when assayed for assembly-stimulated GTPase activity with the use of either microtubules as the assembly template (Figure 2B) or excess GED to mimic self-assembly, neither dyn(S45N) nor dyn(T65F) showed appreciable activity (<1% of WT). Thus, as predicted, each of these mutants was potently defective in both basal and stimulated rates of GTP hydrolysis.

Guanine Nucleotide-binding Rates

Based on analogy to other GTPase superfamily members, we would predict that dyn(S45N) would be preferentially stabilized in the GDP-bound state, whereas dyn(T65F) would

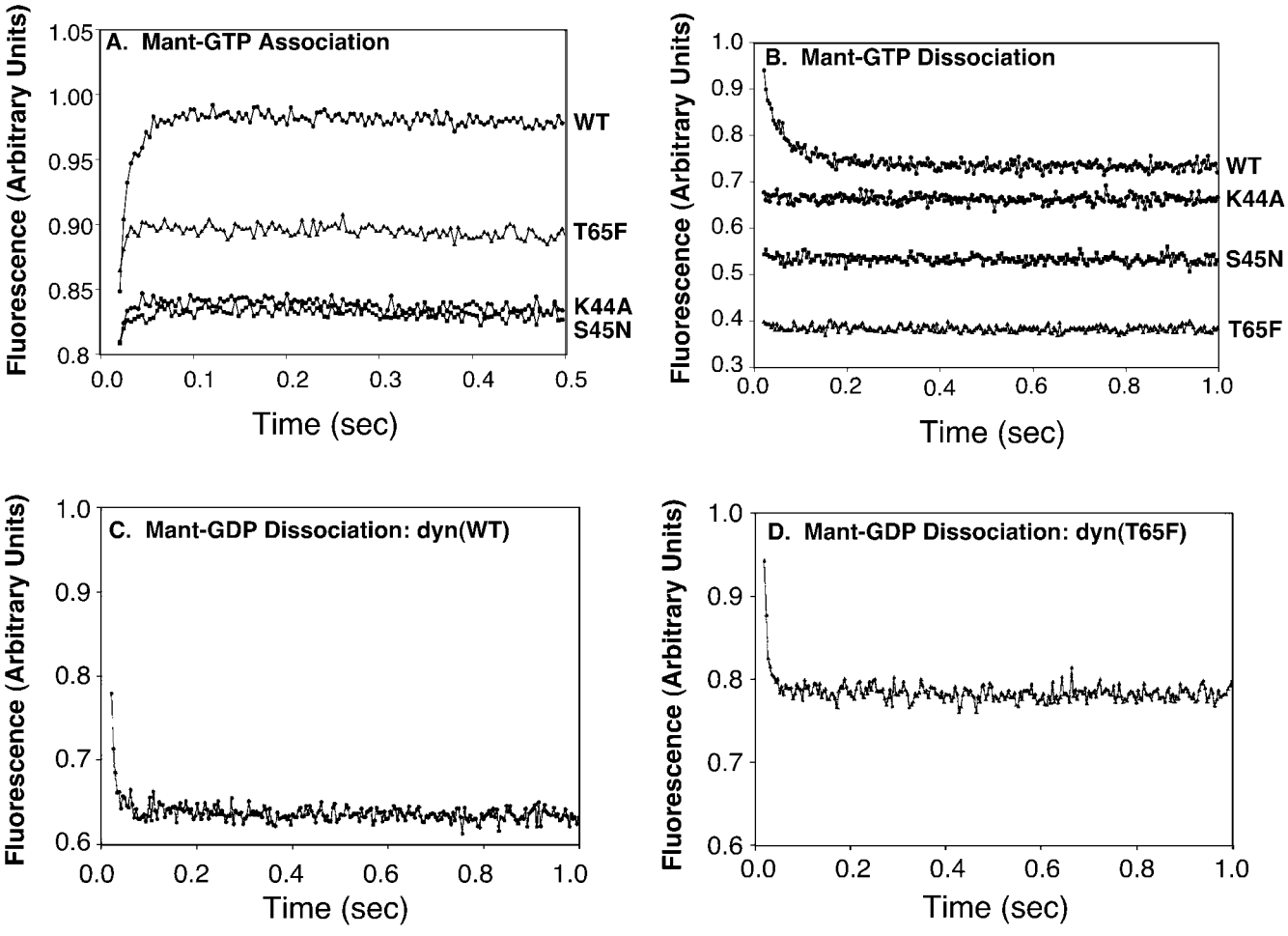

Figure 3. Guanine nucleotide association and dissociation from WT and mutant dyns. Mant-GTP association (A) and dissociation (B) are plotted in arbitrary units for fluorescence over time. In A, WT and mutant dyn-1 (1 μM final concentration) were mixed with Mant-GTP (60 μM final concentration). In B, 1 μM dyn-1 and 4.0 μM Mant-GTP were mixed with 100 μM unlabeled GTP (final concentrations). Mant-GDP dissociation rates were measured by mixing 1 μM dyn(WT) (C) and dyn(T65F) (D) loaded with 4 μM Mant-GDP with 100 μM GTP (final concentrations). See MATERIALS AND METHODS for experimental details.

be preferentially stabilized in the GTP-bound form. To determine how the introduced point mutations affect the nucleotide on and off rates for dyn, stop-flow measurements were performed. For recombinant dyn(WT), we were able to measure the GTP on rate for four concentrations (10, 20, 40, and 60 μM) of 2′deoxy-3′*O*-*N*-methylanthraniloyl GTP (Mant-GTP) at a constant dyn concentration of 1 μM. Analysis of these data gave the same result for the second-order association constant of dyn(WT) with Mant-GTP (7.4×10^5 M^{-1} s^{-1}) as previously published (Binns *et al.*, 1999, 2000) for native dyn-1, purified from bovine brain. In contrast, with the use of the same experimental system it was not possible to determine the GTP on rate for dyn(K44A), dyn(S45N), or dyn(T65F). The association curves for the four proteins (WT, K44A, S45N, and T65F) were plotted in arbitrary fluorescence units (Figure 3A). Importantly, because we do not know the fluorescence intensity change expected for each mutant protein, we cannot correlate intensity changes with nucleotide binding. However, for all three mutants, the amplitude of the reaction was greatly decreased at the same instrument settings, protein concentration, and Mant-GTP concentrations when compared with dyn(WT). These data are consistent with our prediction that dyn(K44A) and dyn(S45N) are defective in GTP binding. In contrast to our prediction, although dyn(T65F) retains some ability to bind GTP, this association appears to be reduced relative to dyn(WT). We attempted to measure GTP off rates (Figure 3B), but only the WT protein was measurable and gave results similar to measurements on native dyn-1 (Binns *et al.*, 1999). The GTP off rates for the other mutants were either too fast for our equipment to measure or negligible at the GTP concentrations used. A higher GTP concentration could not be used because we were exciting at 280 nm and reading the fluorescence emission. The absorption of GTP at 260 nm became significant at higher GTP concentrations.

We next examined the association/dissociation rates for GDP. As reported earlier for native dyn-1 (Binns *et al.*, 1999), the GDP on rates could not be measured for any of the four

proteins because the interaction between dyn and 2′deoxy-3′*O*-*N*-methylanthraniloyl GDP (Mant-GDP) proved either negligible or too fast. The GDP off rates for dyn(WT) and dyn(T65F) were, however, measurable with the use of a competition assay as shown in Figure 3, C and D. For these reactions, one syringe was loaded with 2.0 μM protein and 8.0 μM Mant-GDP, and the other was loaded with 200 μM unlabeled GTP. An equal volume was injected from each syringe into the cuvette, which was excited as described above. This brought the final protein concentration to 1 μM, the final Mant-GDP concentration to 4 μM, and the final GTP (unlabeled) concentration to 100 μM. With this approach we determined that the GDP off rate for dyn(WT) was 92 $\pm$ 12 s^{-1} and for dyn(T65F) it was 151 $\pm$ 18.4 s^{-1}. The value obtained for dyn(K44A), 189 $\pm$ 60 s^{-1}, was very rapid and the SDs were high; thus this value is the least reliable (not shown). Similarly, the dyn(S45N) was either too fast for our equipment to measure or negligible at the Mant-GDP concentration used (not shown). Together these data suggest that, contrary to our predictions, it is unlikely that either dyn(S45N) or dyn(T65F) would be restricted to the GDP- or GTP-bound states, respectively, in vivo. Indeed, all of the dyn GTPase domain mutants we have tested are significantly impaired in nucleotide binding.

Tfn Internalization Is Inhibited in Cells Stably Expressing dyn(S45N) and dyn(T65F)

Stably transformed cell lines expressing either WT dyn or the GTPase domain mutants under control of the tet-regulatable promotor were generated to allow for detailed biochemical and morphological characterization of their endocytic phenotype. Expression of dyn(WT), dyn(K44A), dyn(S45N), or dyn(T65F) was induced in stably transformed tTA-HeLa cells for 48 h by removal of tet (Figure 4, inset). Internalization of Tfn, which is biotinylated via a cleavable disulfide bond (BSS-Tfn), was measured by incubating the cells with 8 μg/ml BSS-Tfn for the indicated times at 37°C. Intracellular Tfn was quantified based on its inaccessibility to the bulky probe avidin (Figure 4A) or its resistance to the small membrane-impermeant reducing agent MesNa (Figure 4B). As can be seen, both dyn(S45N) and dyn(K44A) mutants potently inhibited receptor-mediated endocytosis of BSS-Tfn, by $\geq$ 95%. Overexpression of dyn(T65F) also inhibited receptor-mediated endocytosis but to a lesser extent (~80%). In each of the mutants, BSS-Tfn remained accessible to MesNa and was not sequestered from avidin; therefore, the block occurred before the formation of constricted coated pits.

T65F Is a Weaker Dominant-Negative Mutant than S45N

Dyn(T65F) is strongly defective in GTPase activity; thus, we were intrigued by the fact that its overexpression did not completely inhibit endocytosis. Unlike either dyn(K44A) or dyn(S45N), dyn(T65F) retained some ability, albeit impaired, to bind GTP. Thus, it was possible that the weaker phenotype of dyn(T65F) overexpression might be due to the transient existence of an "activated" GTP-bound form of dyn. Indeed, overexpression of dyn GED mutants that are defective in assembly-stimulated GAP activity, but retain

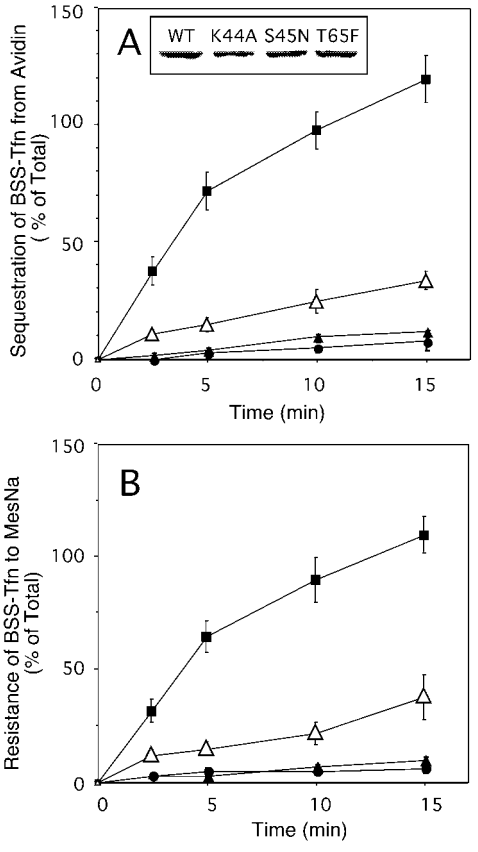

Figure 4. Tfn internalization is inhibited in cells stably expressing dyn(S45N) and dyn(T65F). Stable tTA-HeLa cells expressing WT dyn (■), dyn(K44A) (▲), dyn(S45N) (●), or dyn(T65F) (△) were induced for 48 h by removal of tet. The inset in A indicates the expression levels for exogenous dyn from a single representative assay as analyzed by immunoblotting. Internalization of Tfn was measured by incubating cells with 8 μg/ml BSS-Tfn for the indicated times at 37°C before measuring intracellular Tfn based on its inaccessibility to avidin (A) or MesNa (B) (see MATERIALS AND METHODS). Results are the averages $\pm$ SD of five independent experiments with comparable expression levels for dyn-1.

the ability to bind GTP, stimulates the rate-limiting step in endocytic coated vesicle formation (Sever *et al.*, 1999, 2000a). If this were the case, then the intermediate phenotype we observe might reflect a balance between the inhibitory effect of a dominant-negative mutant and the stimulatory effect of an activated mutant. Such an equilibrium would be independent of expression levels and would lead to an intermediate inhibitory phenotype even at high levels of expression. In contrast, if dyn(T65F) was simply less potent than the other GTPase domain mutants, then higher levels of overexpression should lead to complete inhibition. To distinguish between these two possibilities we generated recombinant Ads expressing dyn(T65F) under the control of the tet promotor. This adenoviral expression system allows for both higher, uniform expression and for tight control of expression levels by varying the amounts of virus and tet. tTA-HeLa cells were infected with Ad (10 MOI/cell) encoding dyn(WT), dyn(K44A), or dyn(T65F) in the absence or

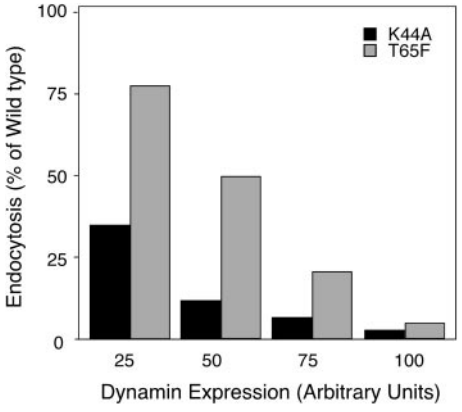

Figure 5. At equal expression levels dyn(T65F) is a weaker inhibitory mutant than dyn(S45N). tTAHela cells were infected with Ad (10 MOI/cell) for WT dyn, dyn(S45N), or dyn(T65F) in the absence or presence of low amounts (2–10 ng/ml) of tet. Cells were processed for internalization of BSS-Tfn and avidin accessibility 16 h after infection as described previously. The expression levels for exogenous dyn were controlled by immunoblot analysis of equal number of cells and quantified by densitometric analysis. Shown are data from four independent experiments. Matching expression levels for HA-dynS45N and T65F of these experiments were plotted versus the percentage of endocytosis. Endocytosis in dyn WT cells at equal expression level is 100%.

presence of low amounts (2–10 ng/ml) of tet. Cells were processed 16 h after infection for internalization of BSS-Tfn with the use of the avidin inaccessibility assay. Expression levels for exogenous dyn were determined by immunoblot analysis of equal numbers of cells and quantified by densitometric analysis. The data in Figure 5 show BSS-Tfn endocytosis as a percentage of that obtained in cells overexpressing dyn(WT) at four matched levels of exogenous protein expression. These data establish that at equal expression levels dyn(T65F) is a weaker inhibitory mutant than dyn(K44A) or dyn(S45N). Nonetheless, at very high levels of overexpression, dyn(T65F) potently inhibits the formation of constricted coated pits. Thus, each of the GTPase domain mutants of dyn acts as a dominant-negative inhibitor of endocytosis.

Morphological Analysis of Coated Profiles in Cells Expressing WT and Mutant Dyns

Our analyses revealed only subtle differences in the enzymological properties among the three dyn GTPase mutants (dyn[K44A], dyn[S45N], and dyn[T65F]) and overexpression of any of these mutants inhibits the formation of constricted coated pits. In an effort to detect new structural intermediates in endocytic clathrin-coated vesicle formation that might reflect subtle functional differences between the dyn mutants, we next carefully compared the morphological intermediates that accumulated in the various mutant cells. tTA-HeLa cells overexpressing dyn(WT), dyn(K44A), dyn(S45N), or dyn(T65F) were incubated with gold-conjugated monoclonal anti-human TfnR antibody (D65-gold, 10 μg/ml) for 2 min at 37°C to uniformly label all endocytic intermediates. The gold labeling allows the easy identification of endocytic coated pits. The representative micrographs in Figure 6 show that there was no significant change

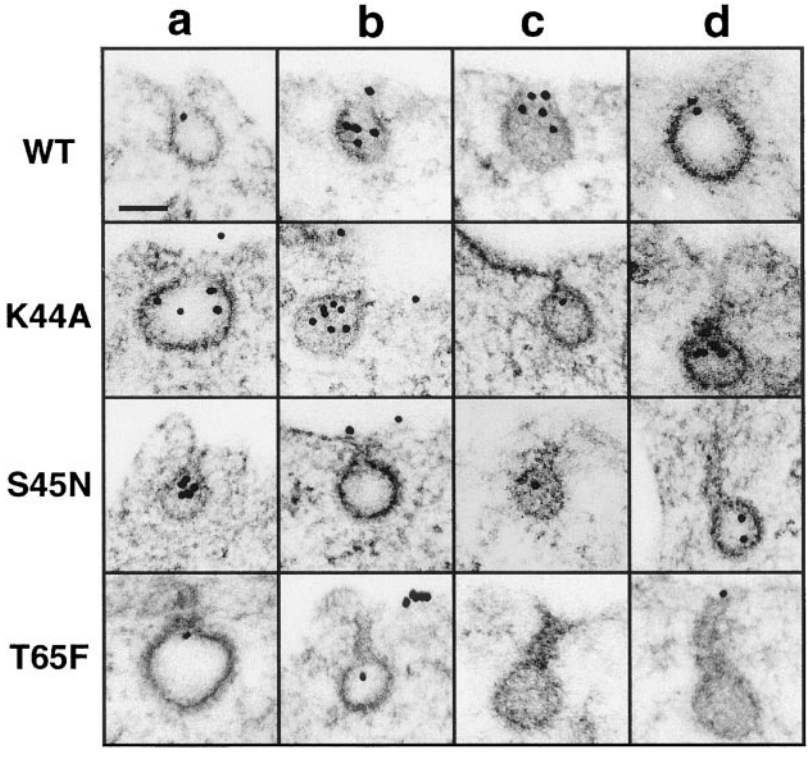

Figure 6. EM analysis of coated profiles in cells expressing WT and mutant dyns. Shown is a gallery of representative deep coated pits from tTA-HeLa cells infected with Ad encoding for dyn(WT), dyn(K44A), dyn(S45N), and dyn(T65F). tTA HeLa cells were infected with 10 MOI of virus in the absence of tet resulting in ≥ 95% of cells expressing dyn. Cells were incubated 16 h after infection with gold-conjugated monoclonal anti-human TfnR antibody (D65-gold, 10 μg/ml) for 2 min at 37°C before fixation, staining, and embedding in Epon for thin-section analysis as described in MATERIALS AND METHODS. Scale bar, 100 nm. The images for WT represent deep pits (a-d). For K44A, the first three images (a–c) are scored as deep pits, whereas the rightmost (D) was scored as elongated, i.e., the neck is longer than the diameter of the pit. For S45N, a and b are deep and c and d are elongated pits. For T65F a is a deep pit, and b–d are elongated pits.

Table 1. Quantification of morphological intermediates of coated pit formation in cells expressing WT and mutant dyns

	Coated Pits		
Cell type	Shallow	Deep	Elongated
WT	4.04 ± 0.94	1.70 ± 0.73	0.03 ± 0.04
Dyn K44A	2.99 ± 0.36	3.39 ± 0.58	0.71 ± 0.26
Dyn S45N	3.11 ± 0.56	2.91 ± 0.27	0.98 ± 0.47
Dyn T65F	2.05 ± 0.57	2.32 ± 0.32	3.81 ± 0.61

Twenty cell profiles with nuclei were randomly selected from cells expressing dyn(WT), dyn(K44A), dyn(S45N), or dyn(T65F). The number of flat and shallow coated pits (i.e., not closing, C-shape but not yet omega-shaped), deep, coated pits (with very short neck, i.e., < 0.25 of pit diameter), and coated pits with elongated neck were directly counted under the EM. At the same time, low magnification (×5000) images of cells were captured with a slow-scan CC camera, and their perimeters were measured using National Institutes of Health image software. The data are shown as the numbers of coated pits per 100 μm length of cell perimeter. The data shown are averages ± S.D. of three independent experiments.

in the morphology or size of individual coated pits or coated vesicles in the cells overexpressing mutant dyns as compared with WT dyn. However, the quantification of multiple cell profiles revealed a morphological difference between the mutants. The results in Table 1 show the number of coated pit intermediates scored as either shallow pits, deeply invaginated pits, or pits observed with elongated necks in cells overexpressing either WT or mutant dyn.

The accumulation of each morphologically distinct intermediate is presented in Figure 7 as a percentage of total coated pits for each mutant. As can be seen, overexpression of each of the dyn mutants caused a pronounced shift from shallow coated pits to deeply invaginated structures as compared with cells overexpressing WT dyn. As expected based on their very similar GTPase- and nucleotide-binding properties in vitro, there was little difference detected between cells overexpressing dyn(K44A) and dyn(S45N). In contrast,

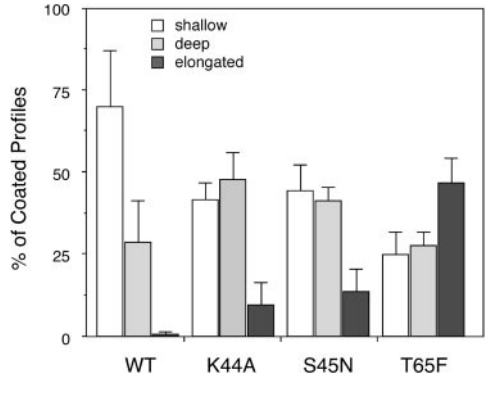

Figure 7. Differential accumulation of endocytic intermediates in cells expressing dyn(K44A), dyn(S45N), or dyn(T65F). Data for various structures derived from the quantitation shown in Table 1 are expressed as percentages of total coated profiles for each condition.

there was a marked accumulation of coated pits with elongated necks in cells overexpressing dyn(T65F), although these structures could also be detected in dyn(K44A)- and dyn(S45N)-expressing cells. In general, the length of the necks was approximately the same size as the diameter of the emerging coated vesicle; however, in some cases very long necks were observed by staining membrane continuities with the use of Ruthenium red (Figure 8A). The differential effects of overexpression of dyn(T65F) were observed both at the highest levels of overexpression obtained in stable tTA-HeLa cells and in cells overexpressing dyn(T65F) driven by recombinant Ad. Although we observed some structures that resembled the collars seen around the necks of endocytic profiles at the nerve terminals in *shibire* flies (Figure 8B), they were very rare. Moreover, these structures were observed in dyn(K44A)-, dyn(S45N)-, and dyn(T65F)-expressing cells and thus we were unable to determine their significance. Importantly, in the case of dyn (T65F)-expressing cells, many of these narrow necks and long tubules remained accessible to gold-labeled anti-TfnR antibody, D65, consistent with our biochemical results establishing that each of the mutants blocked the formation of biochemically defined constricted coated pits (Figure 8B). Thus, quantitative morphological analysis has revealed subtle differences in the effects of overexpression of dyn(T65F) as compared with other dyn GTPase mutants that were not revealed by biochemical analysis.

DISCUSSION

All members of the GTPase superfamily must undergo nucleotide-dependent conformational changes driven by GTP binding and hydrolysis to carry out their role in monitoring complex cellular processes such as protein translation, vesicle formation, or membrane docking and fusion. Overexpression of dominant-negative mutants restricted to either the GDP- or GTP-bound conformations can lead to the accumulation of distinct intermediates in the vectorial processes governed by these GTPases. For example, overexpression of arf6(T27N), which is restricted to the GDP-bound conformation, blocks the recycling of proteins from an endosomal compartment to the plasma membrane, whereas overexpression of arf6(Q67L), which is restricted to the GTP-bound form, blocks endocytosis and delivery of proteins to an endosomal compartment (reviewed by Donaldson and Jackson, 2000). Based on this paradigm, we sought to generate and overexpress dyn mutants restricted to either GDP- or GTP-bound forms to determine the relationship between dyn's GTPase cycle and the complex multistep process of endocytic coated vesicle formation.

Mutations in dyn's GTPase domain were made by analogy to other GTPase superfamily members and were predicted to generate dominant-negative, GDP-bound (S45N) or constitutively active GTP-bound (T65F) dyn mutants. In contrast to our predictions, we found that guanine nucleotide binding in vitro was impaired by each of the mutations we made in the GTPase-binding elements, such that we were unable to generate dyn mutants expected to be restricted to either GDP- or GTP-bound conformations in vivo. Similar consequences of consistently reduced guanine nucleotide-binding affinities have been reported for GTPase domain mutants generated in SRP54 or SRP receptor

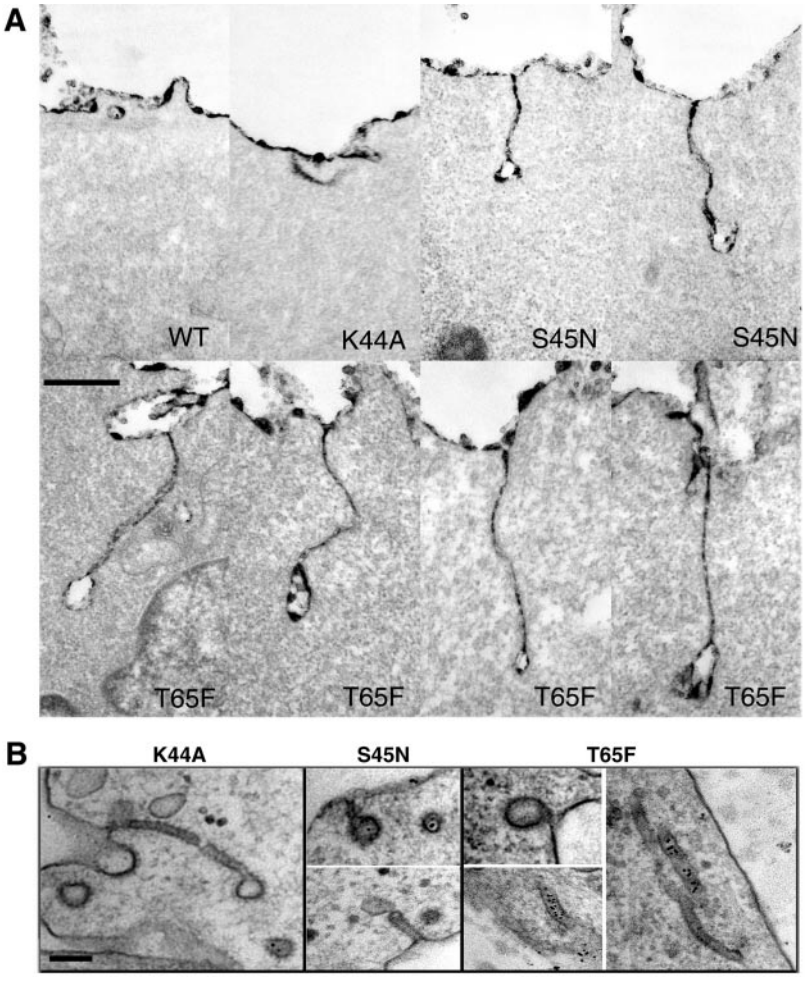

Figure 8. (A) Coated pits with elongated necks accumulate in cells expressing GTPase domain mutant dyns. Ruthenium red staining shows elongated necks that accumulate in mutant cells. For labeling of invaginated membranes with Ruthenium red, tTA-HeLa cells were infected with Ad for WT or mutant dyn-1 and incubated in the absence of tet for 16 h. The cells were fixed in the presence of 0.5 mg/ml Ruthenium red and processed as described in MATERIALS AND METHODS. Scale bar, 500 nm. (B) Shown are some rarely observed examples of necks of elongated coated pits encircled by an electron-dense collar-like material. Whereas such structures were never detected in WT cells, they were observed in cells expressing each of the dyn GTPase domain mutants. These images are taken from stably transformed tTA-HeLa cells induced to express the indicated mutant dyns by removal of tet. Scale bar, 100 nm.

GTPase domains (R. Gilmore, personal communication). As for the dyn family of GTPases, SRP54 and SRP receptor GTPases have a low affinity for nucleotides (~10 μM) relative to the very high affinity (subnanomolar) of ras superfamily GTPases or to G-protein α-subunits. The residues we have mutated, K44, S45, and T65 are invariant among GTPase superfamily members and mutations in these residues in ras-related GTPases or trimeric GTPases have also been shown to reduce the affinity for GTP binding (Wittinghofer, 2000). However, given the very high affinity of these GTPases for GTP and GDP, the reduction in affinity is insignificant in the presence of physiological concentrations of nucleotides. By contrast, further reduction of the already low affinity of dyn family GTPases appears to significantly perturb their ability to bind GTP or GDP under physiological conditions. Our results emphasize the importance of isolating mutant proteins and evaluating their enzymological characteristics to confirm predictions regarding their phenotypic properties.

Consistent with our inability to distinguish the biochemical characteristics of dyn(K44A) and dyn(S45N) in vitro, the effects of overexpression of either of these mutants on receptor-mediated endocytosis in vivo were also indistinguishable. Moreover, extensive morphological characterization of cells overexpressing these mutants revealed that, although significantly shifted toward more invaginated coated pits than in cells expressing WT dyn, the coated endocytic structures that accumulated were quite pleiomorphic. Some had short necks, some had long, thin necks, and, on very rare occasions (in cells expressing either of the GTPase domain mutants), we detected narrow necks encircled by electron-dense material. Inhibition by dominant-negative and constitutively active mutants of GTPase superfamily members is believed to be due to sequestration of upstream and downstream effectors (Olkkonen and Stenmark, 1997; Wittinghofer, 2000). Because the dyn mutants we have generated are not locked in GDP- or GTP-bound states, they are unlikely to effectively interact with effector molecules, perhaps accounting for the pleiomorphic nature of the coated endocytic profiles that accumulate.

Our observations with the dyn(T65F) mutant were also unexpected and somewhat paradoxical. Dyn(T65F), as predicted, exhibited little or no detectable GTPase activity, and yet it was a less potent dominant-negative mutant of receptor-mediated endocytosis than dyn(K44A) or dyn(S45N). Our results ruled out the possibility that this reduced potency was due to partially functional, transiently existing GTP-bound forms of dyn(T65F). A more likely explanation

to the reduced potency of dyn(T65F) mutants can again be derived by comparison with other GTPase superfamily members. Thr65 is an invariant residue located in the switch 1 region of the GTP domain that coordinates with Mg^{2+}, which, in turn, coordinates with the γ-phosphate when GTP is bound in the active site. Substitution of the conserved Thr in ras-related proteins reduces their affinity for GTP (Wittinghofer, 2000), but the more important functional consequence lies in the fact that the repositioning of this Thr in response to GTP binding results in conformational changes in the loop 2, effector-binding region of the GTPase domain (Bourne *et al.*, 1990) and is required for GTP-dependent interaction with downstream effectors. Thus, the weaker phenotype of dyn(T65F) most likely reflects the fact that this mutant is unable to undergo the GTP-bound conformational change needed for interaction of effectors with the dyn GTPase domain effector loop. Its inability to adopt the GTP-bound conformation might account for its reduced potency as a dominant-negative mutant, and/or its inability to act as an activating mutant.

During the course of our studies, others have recently reported that dyn(T65A) is a potent inhibitor of receptor-mediated endocytosis (Hill *et al.*, 2001; Marks *et al.*, 2001). These findings are most likely consistent with our results with dyn(T65F) because it is difficult to assess the levels of overexpression in transient transfection experiments. It is also possible that substitution of Thr65 with Ala rather than Phe allows greater conformational flexibility in the switch 1 region and that the T65A mutation is, in fact, more potent than T65F. We chose a bulkier residue to prevent the possibility of a water molecule being positioned to coordinate with the Mg^{2+}. In contrast to our findings for dyn(T65F), it has also been reported that dyn(T65A) binds GTP with comparable affinity to WT dyn (Marks *et al.*, 2001). In these studies GTP-binding affinities were not measured directly and instead were determined based on K_m values obtained for the very low residual GTPase activity. However, these authors also reported that dyn(T65A) failed to adopt the tight, ordered spirals obtained with WT dyn, when assembled around liposomes in the presence of GTPγS (Marks *et al.*, 2001). This latter result is consistent with our suggestion that dyn(T65) mutants, like analogous mutations in other GTPase superfamily members, fail to adopt the GTP-bound, activated conformation. Moreover, the observed inhibitory effects of dyn(T65A) on endocytosis are also consistent with our suggestion that dyn(T65) mutants do not correspond to the activating mutants of other GTPase superfamily members.

All three inactivating dyn mutants blocked receptor-mediated endocytosis at a stage preceding the formation of avidin-inaccessible, constricted coated pits. This is the same step that is accelerated by dyn GED mutants (Sever *et al.*, 2000a), suggesting that it is the key event dependent on dyn function. Quantitative morphological analysis revealed that coated profiles accumulating in cells overexpressing dyn(T65F) tended to have longer, narrow necks relative to those detected in dyn(K44A)- or dyn(S45N)-expressing cells. Although it is attractive to speculate that these represent later intermediates in the formation of endocytic coated vesicles, we have no way of distinguishing whether these are bona fide intermediates or aberrant structures i.e., elongated necks, such as these, are seldom observed in untreated cells. In contrast to observations in cells overexpressing dyn(T65A) (Marks *et al.*, 2001), we did not generally detect electron-dense collars on these elongated necks. It has been reported that other proteins must be recruited to membrane tubules before dyn spirals can be detectable by thin-section EM (Takei *et al.*, 1999). Thus, our inability to detect assembled dyn spirals in vivo may reflect the inability of dyn(T65F) to undergo a conformational change necessary for efficient recruitment of downstream effectors.

All GTPase superfamily members must be able to bind and hydrolyze GTP and to adopt distinct conformations in their GTP- and GDP-bound forms to mediate their cellular function, typically through nucleotide-dependent interactions with upstream and downstream effector molecules. Here we report that three distinct GTPase domain mutants of dyn function as dominant-negative inhibitors of receptor-mediated endocytosis. These results, and those of others (Herskovits *et al.*, 1993; van der Bliek *et al.*, 1993; Hill *et al.*, 2001; Marks *et al.*, 2001), clearly establish that GTP binding and hydrolysis is also essential for dyn function in vivo. How can these results be reconciled with previous reports (Sever *et al.*, 1999, 2000a) that GAP-impaired GED mutants of dyn stimulate specific steps in receptor-mediated endocytosis? In fact, we do not view these results as contradictory. Importantly, all of the GTPase domain mutants that we have generated have undetectable basal rates of GTP hydrolysis and are defective in GTP and GDP binding in vitro and/or are unable to adopt an activated GTP-bound conformation. In contrast, mutations in GED perturb the assembly-stimulated GAP activity but do not effect the function of the GTPase domain. Dyn GED mutants maintain their basal rate of GTP hydrolysis, their ability to bind GTP, and their ability to productively interact with upstream and downstream effectors. Thus, unlike the GTPase domain mutants so far analyzed, the dyn GED mutants can adopt an activated state. This interpretation is consistent with our observations that GED mutants stimulate events in endocytic vesicle formation, whereas GTPase domain mutants are inhibitory. Recent findings regarding the antiviral function of the dyn-related protein, Mx, are completely consistent with this interpretation. Mutations in the GTPase domain of Mx that abrogate GTPase activity disrupt the protein's ability to confer viral resistance (Ponten *et al.*, 1997). In contrast, an Mx protein carrying a mutation in its GAP/assembly domain that abrogates both self-assembly and GTPase activity retains its antiviral activity (Janzen *et al.*, 2000). Thus, for both dyn and Mx proteins, their assembly-activated GAP activities are apparently not required for cellular function.

Recent results identified a new dyn GTPase domain mutant, dyn(K142A), which hydrolyzes GTP at near WT rates but is defective in undergoing a GTP hydrolysis-driven conformational change (Marks *et al.*, 2001). Dyn(K142A) also functions as a dominant-negative inhibitor of endocytosis, providing strong evidence for the importance of GTP-driven conformational changes for dyn function in vivo. Importantly, the requirements for GTP binding and hydrolysis and for GTP-dependent conformational changes do not distinguish between models for dyn function as either a regulatory or mechanochemical GTPase. New approaches and new mutants are needed to distinguish between the prevailing models for dyn's function in endocytic coated vesicle formation.

ACKNOWLEDGMENTS

We thank Miya Fujimoto for technical assistance and Richard Jacobs (Salk Institute) for skilled preparation of serial sections and EM. We thank Joe Albanesi and John Heuser for helpful discussions and members of the Schmid laboratory for their many contributions. With the assistance of Chris Hofeditz, extensive use was made of the EM Core Facility led by Dr. M. Farquhar under the auspices of National Cancer Institute grant CA58689. H.D. was supported by California Cancer Research Program 00-00743V-20070 and S.L.S. was supported by National Institutes of Health grant GM42455. This is The Scripts Research Institute manuscript 13994-CB. This publication was made possible by funds received from the Cancer Research Fund, under Interagency Agreement 97-12013 (University of California, Davis contract 98-00924V) with the Department of Health Services, Cancer Research Section.

REFERENCES

Altschuler, Y., Barbas, S., Terlecky, L., Mostov, K., and Schmid, S.L. (1998). Common and distinct functions for dynamin-1 and dynamin-2 isoforms. J. Cell Biol. *143*, 1871–1881.

Barylko, B., Binns, D., Lin, K.M., Atkinson, M.A., Jameson, D.M., Yin, H.L., and Albanesi, J.P. (1998). Synergistic activation of dynamin GTPase by Grb2 and phosphoinositides. J. Biol. Chem. *273*, 3791–3797.

Binns, D.D., Barylko, B., Grichine, N., Adkinson, A.L., Helms, M.K., Jameson, D.M., Eccleston, J.F., and Albanesi, J.P. (1999). Correlation between self-association modes and GTPase activation of dynamin. J. Protein Chem. *18*, 277–290.

Binns, D.D., Helms, M.K., Barylko, B., Davis, C.T., Jameson, D.M., Albanesi, J.P., and Eccleston, J.F. (2000). The mechanism of GTP hydrolysis by dynamin II: a transient kinetic study. Biochemistry *39*, 7188–7196.

Bourne, H.R., Sanders, D.A., and McCormick, F. (1990). The GTPase superfamily: a conserved switch for diverse cell functions. Nature *348*, 125–132.

Bourne, H.R., Sanders, D.A., and McCormick, F. (1991). The GTPase superfamily: conserved structure and molecular mechanism. Nature *349*, 117–127.

Carter, L.L., Redelmeier, T.E., Woollenweber, L.A., and Schmid, S.L. (1993). Multiple GTP-binding proteins participate in clathrin-coated vesicle-mediate endocytosis. J. Cell Biol. *120*, 37–45.

Damke, H., Baba, T., van der Bliek, A.M., and Schmid, S.L. (1995a). Clathrin-independent pinocytosis is induced in cells overexpressing a temperature-sensitive mutant of dynamin. J. Cell Biol. *131*, 69–80.

Damke, H., Baba, T., Warnock, D.E., and Schmid, S.L. (1994). Induction of mutant dynamin specifically blocks endocytic coated vesicle formation. J. Cell Biol. *127*, 915–934.

Damke, H., Freundlieb, S., Gossen, M., Bujard, H., and Schmid, S.L. (1995b). Tightly regulated and inducible expression of a dominant interfering dynamin mutant in stably transformed HeLa cells. Methods Enzymol. *257*, 209–221.

Damke, H., Muhlberg, A.B., Sever, S., Sholly, S., Warnock, D.E., and Schmid, S.L. (2001). Expression, purification, and functional assays for self-association of dynamin-1. Methods Enzymol. *329*, 447–457.

Donaldson, J.G., and Jackson, C.L. (2000). Regulators and effectors of ARF GTPases. Curr. Opin. Cell Biol. *12*, 475–482.

Gossen, M., and Bujard, H. (1992). Tight control of gene expression in mammalian cells by tetracycline-responsive promoters. Proc. Natl. Acad. Sci. USA *89*, 5547–5551.

Hardy, S., Kitamura, M., Harris-Stansil, T., Dai, Y., and Phipps, M.L. (1997). Construction of adenovirus vectors through Cre-*lox* recombination. J. Virol. *71*, 1842–1849.

Herskovits, J.S., Burgess, C.C., Obar, R.A., and Vallee, R.B. (1993). Effects of mutant rat dynamin on endocytosis. J. Cell Biol. *122*, 565–578.

Hill, E., van der Kaay, J., Downes, C.P., and Smythe, E. (2001). The role fo dynamin and its binding partners in coated pit invagination and scission. J. Cell Biol. *152*, 309–324.

Hinshaw, J.E. (2000). Dynamin and Its Role in Membrane Fission. Annu. Rev. Cell Dev. Biol. *16*, 483–519.

Hinshaw, J.E., and Schmid, S.L. (1995). Dynamin self assembles into rings suggesting a mechanism for coated vesicle budding. Nature *374*, 190–192.

Janzen, C., Kochs, G., and Haller, O. (2000). A monomeric GTPase-negative MxA mutant with antiviral activity. J. Virol. *74*, 8202–8206.

Kirchhausen, T. (1999). Adaptors for clathrin-mediated traffic. Annu. Rev. Cell Dev. Biol. *15*, 705–32.

Kirchhausen, T. (2000). Clathrin. Annu. Rev. Biochem. *69*, 699–727.

Koenig, J.H., and Ikeda, K. (1989). Disappearance and reformation of synaptic vesicle membrane upon transmitter release observed under reversible blockage of membrane retrieval. J. Neurosci. *9*, 3844–3860.

Kozlov, M.M. (2001). Fission of biological membranes: interplay between dynamin and lipids. Traffic *2*, 51–65.

Leunissen, J.L.M., and DeMey, J.R. (1987). Preparation of Gold Probes, Boca Raton, FL: CRC Press, 3–16.

Maeda, K., Nakata, T., Noda, Y., Sato-Yoshitake, R., and Hirokawa, N. (1992). Interaction of dynamin with microtubules: its structure and GTPase activity investigated by using highly purified dynamin. Mol. Biol. Cell *3*, 1181–1194.

Marks, B., Stowell, M.H.B., Vallis, Y., Mills, I.G., Gibson, A., Hopkins, C.R., and McMahon, H.T. (2001). GTPase activity of dynamin and resulting conformation change are essential for endocytosis. Nature *410*, 231–235.

McNiven, M.A. (1998). Dynamin: a molecular motor with pinchase action. Cell *94*, 151–154.

Olkkonen, V.M., and Stenmark, H. (1997). Role of Rab GTPases in membrane traffic. Int. Rev. Cytol. *176*, 1–85.

Ponten, A., Sick, C., Weeber, M., Haller, O., and Kochs, G. (1997). Dominant-negative mutants of human MxA protein: domains in the carboxy-terminal moiety are important for oligomerization and antiviral activity. J. Virol. *71*, 2591–2599.

Roos, J., and Kelly, R. (1997). Is dynamin really a 'pinchase.' Trends Cell Biol. *7*, 257–259.

Schmid, S.L. (1997). Clathrin-coated vesicle formation and protein sorting: an integrated process. Annu. Rev. Biochem. *66*, 511–548.

Sever, S., Damke, H., and Schmid, S.L. (2000a). Dynamin:GTP controls the formation of constricted coated pits, the rate limiting step in clathrin-mediated endocytosis. J. Cell Biol. *150*, 1137–1148.

Sever, S., Damke, H., and Schmid, S.L. (2000b). Garrotes, springs, ratchets and whips: putting dynamin models to the test. Traffic *1*, 385–392.

Sever, S., Muhlberg, A.B., and Schmid, S.L. (1999). Impairment of dynamin's GAP domain stimulates receptor-mediated endocytosis. Nature *398*, 481–486.

Shpetner, H.S., and Vallee, R.B. (1989). Identification of dynamin, a novel mechanochemical enzyme that mediates interactions between microtubules. Cell *59*, 421–432.

Shupliakov, O., Low, P., Grabs, D., Gad, H., Chen, H., David, C., Takei, K., De Camilli, P., and Brodin, L. (1997). Synaptic vesicle endocytosis impaired by disruption of dynamin-SH3 domain interactions. Science *276*, 259–263.

Smirnova, E., Shurland, D.L., Newman-Smith, E.D., Pishvaee, B., and van der Bliek, A.M. (1999). A model for dynamin self-assembly based on binding between three different protein domains. J. Biol. Chem. *274*, 14942–14947.

Smythe, E., Redelmeier, T.E., and Schmid, S.L. (1992). Receptor-mediated endocytosis in semiintact cells. Methods Enzymol. *219*, 223–234.

Stowell, M.H.B., Marks, B., Wigge, P., and McMahon, H.T. (1999). Nucleotide-dependent conformational changes in dynamin: evidence for a mechanochemical molecular spring. Nat. Cell Biol. *1*, 27–32.

Sweitzer, S., and Hinshaw, J. (1998). Dynamin undergoes a GTP-dependent conformational change causing vesiculation. Cell *93*, 1021–1029.

Takei, K., Slepnev, V.I., Haucke, V., and De Camilli, P. (1999). Functional partnership between amphiphysin and dynamin in clathrin-mediated endocytosis. Nat. Cell Biol. *1*, 33–39.

Tuma, P.L., and Collins, C.A. (1994). Activation of dynamin GTPase is a result of positive cooperativity. J. Biol. Chem. *269*, 30842–30847.

van der Bliek, A.M. (1999). Functional diversity in the dynamin family. Trends Cell Biol. *9*, 96–102.

van der Bliek, A.M., Redelmeier, T.E., Damke, H., Tisdale, E.J., Meyerowitz, E.M., and Schmid, S.L. (1993). Mutations in human dynamin block an intermediate stage in coated vesicle formation. J. Cell Biol. *122*, 553–563.

Warnock, D.E., Baba, T., and Schmid, S.L. (1997). Ubiquitously expressed dynamin-II has a higher intrinsic GTPase activity and a greater propensity for self-assembly than neuronal dynamin-I. Mol. Biol. Cell *8*, 2553–2562.

Warnock, D.E., Hinshaw, J.E., and Schmid, S.L. (1996). Dynamin self assembly stimulates its GTPase activity. J. Biol. Chem. *271*, 22310–22314.

Warnock, D.E., and Schmid, S.L. (1996). Dynamin GTPase, a force generating molecular switch. Bioessays *18*, 885–893.

Warnock, D.E., Terlecky, L.J., and Schmid, S.L. (1995). Dynamin GTPase is stimulated by crosslinking through the C terminal proline rich domain. EMBO J. *14*, 1322–1328.

Wittinghofer, A. (2000). The functioning of molecular switches in three dimensions. In: GTPases, Vol. 24, A. Hall, ed., New York: Oxford University Press,. 244–310.